Mechanics of Advanced Composite Structures 7 (2020) 49 – 58

Semnan University

Mechanics of Advanced Composite Structures

journal homepage: http://MACS.journals.semnan.ac.ir

Vibration Characteristics of Functionally Graded Micro-Beam Carrying an Attached Mass

A. Rahmani[a], A. Babaei[b], S. Faroughi[a,*]

[a] *Faculty of Mechanical Engineering, Urmia University of Technology, Urmia, Iran*
[b] *Department of Mechanical Engineering, University of Kentucky, Lexington, KY, 40506, USA*

KEYWORDS

FG bio-micro-beam
Vibration analysis
Modified couple stress theory
Non-dimensional frequency
Biological and biomedical application of bio-micro-systems

ABSTRACT

In this article, in reference to the modified couple stress theory and Euler-Bernoulli beam theory, the free lateral vibration response of a micro-beam carrying a moveable attached mass is investigated. This is a decent model for biological and biomedical applications beneficial to the early-stage diagnosis of diseases and malfunctions of human body organs and enzymes. The micro-cantilever beam is composed of functionally graded materials (FGMs). The material properties are supposed to show variations through-thickness of the beam in consonance to the power of law. Rayleigh-Ritz method is applied in order to explore the natural frequencies of the first three vibration modes. In order to manifest the accuracy of the proposed method, the results are established and juxtaposed with technical literature. Influences of the material length-scale parameter that captures the size-dependency, ratio of the mass of the beam to the mass of the attached mass and power index of the graded material consequent to the vibrational behavior of the system are contemplated. This technical research denotes the value of the material gradation besides to the inertia of an attached mass in the dynamic behavior of the bio-micro-systems. As a result, the adoption of suitable power index, mass ratio and position of the attached mass lead to the superior design of bio-micro-systems persuading early-stage diagnostics.

1. Introduction

Functionally graded materials (FGMs) can be interpreted as non-homogeneous graded composites consisted of a mixture of two different materials, usually a metal and a non-metal phase. They dominate the desired continuous variation of mechanical properties as a function of position, in accordance with a certain direction(s). These types of materials are constructed in order to exploit the specific benefits of both constituents. Recently, FGMs are widely applied in micro-structures such as thin films in the form of shape memory alloys, micro-electro-mechanical-systems (MEMS), nano-electro-mechanical-systems (NEMS) and atomic force microscopes (AFMs)[1].

By the compelling improvements contributing to micro-technology, consisted of concepts, modeling, design, and fabrication, a micro-cantilever beam that has the dimensions at the order of micron has been widely applied. The applications chiefly include atomic force microscopes (AFMs), micro and nano-electro-mechanical systems (MEMS, NEMS). Micro-electro-mechanical Systems mainly arranged by miniaturized electro-mechanical and mechanical elements. In the mentioned technology, the elements are being engendered applying the microfabrication techniques. Micro-sensors and micro-actuators are among the most beneficial and pragmatic elements of MEMS [2]. As the structure is scaled down, the size effect phenomena influence the dynamic responses directly. It is experimentally illustrated that the size-dependency of microstructures could not be captured by the classical elasticity theory, consequently non-classical elasticity theories emerge. The modified couple stress theory as one of these non-classical theories, contemplating the rotational characteristics that exert the rotational energy terms into the formulations of energy. By applying a single material length scale parameter, symmetric part of the curvature tensor, it becomes correlated to the couple stress tensor; further this correlation makes the modified

* Corresponding author. Tel.: +989126229057
E-mail address: sh.farughi@uut.ac.ir

DOI: 10.22075/MACS.2019.18186.1214
Received 2019-07-03; Received in revised form 2019-09-03; Accepted 2019-11-14

couple stress theory as one of the most prevalent non-classical theories for investigation of the micro-structures. Several researchers have inspected the static and dynamic behavior of FGM beams and plates. Babaei and Yang [3]accomplished research related to vibration analysis of rotating rods with applications in MEMS-gyroscopes. They have proposed a novel modified coupled displacement fields optimizing the design of micro-systems in the industry of automotive. Babaei and Ahmadi [4] reported dynamic characteristics of a non-uniform and non-homogenous micro-model of a Timoshenko beam pursuant to the modified couple stress theory (MCST). For the first time, Babaei and Rahmani [5] considered the capricious model of the non-classical length-scale parameter. Moreover, variations impact over dynamic-vibration behavior is revealed as well. Babaei et al. [6] explored the thermal stress effect over the dynamic characteristics of MEMS. They deliberated various slenderness ratios in order to cover a wide range of applications. Babaei [7] proposed an optimized model of MEMS-gyroscope based on his novel modified coupled displacement kinematic field. He presents perceptible and chaotic patterns of the gyroscope that ameliorates the efficiency of navigation systems mostly applied in advanced cars and airplanes. Chen et al. [8] proposed a new method for free vibration of generally laminated beams based on the state-space-based differential quadrature method. Xiang and Yang [9] inspected free and forced vibration of a laminated FG beam of variable thickness with thermal initial stresses. The effect of diverse boundary conditions was inquired and the beam was presumed to be subjected to one-dimensional steady heat conduction in the thickness direction before undergoing any dynamic deformation. Elastic behavior of FGM ultra-thin films is surveyed by Lü et al. [[10]. They proposed a generalized theory pondered the surface effects in order to capture the size-dependency of the structure's responses. Amar et al. [11] examined the free vibration analysis of the Euler-Bernoulli beam applying the modified couple stress theory. Pradhan and Chakraverty [12] did research on free vibration analysis of Timoshenko and Euler beams. They used functionally graded materials for modeling their systems and applied the Rayleigh-Ritz method for solution procedure. Aghazadeh et al. [13] investigated the free vibration and static behavior of small scale FG micro-beams using dissimilar beam theories and the modified couple stress theory. Additionally, they assumed the varying length scale parameter and its effects consequent to the tip deflection and frequency characteristics. Jafari et al. [14] inquired about the bending and vibration analysis of delaminated micro-beams regarding the modified couple stress theory. They utilized the presumed modes method for analysis. Ansari et al. [15] inspected on the free vibration behavior of FG micro-beams applying the strain gradient theory and the Timoshenko beam theory. They attempted to simulate a model including the thick micro-beams theories. The paper which reported the size-dependent behavior of the FG Euler-Bernoulli micro-cantilever beam, using the modified couples stress theory is accomplished by Asghari et al. [16]. Ansari et al. [17] carried out research concerning buckling and vibrations of micro-plates employing the strain gradient theory. Babaei et al. [18] proposed a micro-beam model considering variations of both temperature and material gradation based on modified couple stress and the Euler-Bernoulli beam theories. Shafiei et al. [19] conducted research about size-dependent vibration analysis of non-uniform FG micro-beam. They have assumed Euler-Bernoulli and Timoshenko beam theories for deriving the formulas. Ansari et al. [20] inquired the vibration of postbuckle piezoelectric micro-beams applying non-local theory. Farajpour et al. [21] investigated the nonlinear behavior of nano-tubes conveying nanofluid with both subcritical and supercritical regimes. They presented the model established based on strain gradient theory. Mohammadimehr et al. [22] reported Size-dependent Effects on the Vibration Behavior of a Timoshenko Microbeam subjected to Pre-stress Loading based on DQM. Arabghahestani and Karimian [23] developed the previous research with considerations of uniform liquid argon flow. Fang et al. [24] represented a size-dependent vibration analysis of rotating small-scaled beam. They exployed the modified couple stress theory in order to devisethe formulations along with smooth variations of the mechanical properties. Khaniki and Rajasekaran [25] carried out a research regarding to vibrational behavior of bi-directional non-uniform beams based on MCST. Jia et al. [26] explored mechanical buckling behavior of small-scaled beams based on MCST under thermal and electrical loads. Their model is supposed to be functionally graded.

In this paper, a functionally graded micro-scale Euler-Bernoulli beam model is proposed for the size-dependent free vibration analysis. This model is presented as a biomedical and biological laboratory set-up to help diagnosis of diseases and detecting body and enzyme malfunctions. It is noteworthy to mention that the said attached mass (proof mass) represents blood or enzyme samples. In order to extend the research available in the literature, the present analysis includes investigation of the influences of inertia generated as a result of the oscillation of the attached mass and varying position of the mass consequent to frequencies of the micro-cantilever beam. The kinetic and strain energy are derived from employing the modified couple stress theory. Due to the usage of the Rayleigh-Ritz method, applying variational approaches is not required. The influences of the volume fraction profiles of the constituents and gradient index (power index) upon the natural frequencies of the micro-cantilever beam are reported.

2. Functionally Graded Material

A functionally graded micro-beam is illustrated in Figure 1, where length is L, width is b and thickness is h . The Cartesian coordinates are defined as $x = x_1, y = x_2, z = x_3$ in correspondence to the length, width and thickness directions. The FG micro-beam is formed by Steel (a metal constituent) and Alumina (a non-metal constituent). It is postulated that the effective mechanical properties vary through the thickness direction (x_3).

Pursuant to the rule of mixtures, the effective properties (P) can be computed as follows:

$$P = P_a V_a + P_s V_s \tag{1}$$

where P_a and P_s represent the effective mechanical properties, V_a and V_s are the volume fractions of alumina and steel phases. The Volume fractions are constrained by the following equation:

$$V_a + V_s = 1 \tag{2}$$

It is postulated that the effective material properties of the FG micro-beam are numerically interpreted by a power-law. The volume fraction of the alumina is defined as Wakashima [46]:

$$V_a = (\frac{z}{h} + \frac{1}{2})^k \tag{3}$$

where k is the power-law exponent, which computes the material variation contour in conformity with thickness direction.

Applying Eqs. (1), (2), and (3), the effective material properties of the FG micro-beam take the form below:

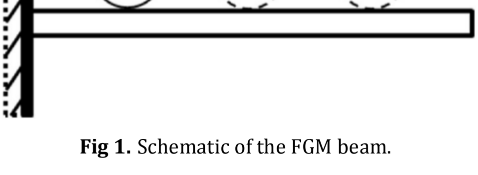

Fig 1. Schematic of the FGM beam.

$$P(z) = (P_a - P_s)\left(\frac{z}{h} + \frac{1}{2}\right)^k + P_s \tag{4}$$

Similarly, Young's modulus, shear modulus and density of the micro-structure structure can be expressed as follows:

$$E(z) = (E_a - E_s)\left(\frac{z}{h} + \frac{1}{2}\right)^k + E_s \tag{5}$$

$$G(z) = (G_a - G_s)\left(\frac{z}{h} + \frac{1}{2}\right)^k + G_s \tag{6}$$

$$\rho(z) = (\rho_a - \rho_s)\left(\frac{z}{h} + \frac{1}{2}\right)^k + \rho_s \tag{7}$$

3. Mathematical Formulation

3.1. *Modified Couple Stress Theory*

Pursuant to the modified couple stress theory developed by Yang et al. [47], the total strain energy of a loaded beam is obtained as follows:

$$U_s = \frac{1}{2}\int_V \left(\sigma_{ij}:\varepsilon_{ij} + m_{ij}:\chi_{ij}\right) dV \tag{8}$$

In Eq. (8), σ_{ij} designates the Cauchy stress, tensor ε_{ij} is the Cauchy strain tensor, m_{ij} represents the deviatoric part of the couple stress tensor and χ_{ij} stands for the symmetric curvature tensor. The tensors ε_{ij} and χ_{ij} are defined by Eqs. (9), (10).

$$\varepsilon_{ij} = \frac{1}{2}\left(u_{i,j} + u_{j,i}\right) \tag{9}$$

$$\chi_{ij} = \frac{1}{2}\left(e_{ipq}\varepsilon_{qj,p} + e_{jpq}\varepsilon_{qi,p}\right) \tag{10}$$

u_i in Eq. (9) shows the displacement vector; e_{ipq} in Eq. (10) denotes00000000 the alternating tensor and comma stand for differentiation. Constitutive relations in reference to the Cauchy stress tensor and the deviatoric part of the couple stress tensor is to be written in the following form:

$$\sigma_{ij} = 2G\varepsilon_{ij} + \lambda\delta_{ij}\varepsilon_{kk} \tag{11}$$

$$m_{ij} = 2Gl^2\chi_{ij} \tag{12}$$

$$\lambda = \frac{E\nu}{(1+\nu)(1-2\nu)} \tag{13}$$

where λ and G are classical Lame parameters. Moreover, ν is the Poisson's ratio, E is Young's modulus and G is shear modulus.

l in Eq. (12) is the material length scale parameter. Employing this non-classical parameter captures the size-dependency of the structure.

3.2. *Euler-Bernoulli beam theory (EBT)*

The general displacement components in a Cartesian coordinate, applying EBT can be expressed as below:

$$u_1(x,z,t) = -z\frac{\partial w}{\partial x} \quad (14)$$

$$u_2(x,z,t) = 0 \quad (15)$$

$$u_3(x,z,t) = w(x,t) \quad (16)$$

In consonance to Eqs. (14)-(16) the elements of ε_{ij}, χ_{ij}, σ_{ij} and m_{ij} are computed as follows:

$$\varepsilon_{11} = -z\frac{\partial^2 w}{\partial x^2} \quad (17)$$

$$\chi_{12} = \chi_{21} = -\frac{1}{2}\frac{\partial^2 w}{\partial x^2} \quad (18)$$

$$\sigma_{11} = -Ez\frac{\partial^2 w}{\partial x^2} \quad (19)$$

$$m_{12} = m_{21} = -Gl^2\frac{\partial^2 w}{\partial x^2} \quad (20)$$

Substitution of Eqs. (17)-(20) into the Eq. (8), shows the strain energy of the Euler-Bernoulli beam:

$$Us = \frac{1}{2}\int_0^L \int_A [\left(\frac{\partial^2 w}{\partial x^2}\right)^2 \begin{pmatrix} E(z)z^2 \\ +\frac{1}{2}G(z)l^2 \end{pmatrix}]dAdx \quad (21)$$

The kinetic energy of the Euler- Bernoulli beam carrying an attached mass can be expressed as follows:

$$T = \frac{1}{2}\int_0^L \rho(z)A\left(\frac{\partial w}{\partial t}\right)^2 dx + \frac{1}{2}M\left(\frac{\partial w(L,t)}{\partial t}\right)^2 \quad (22)$$

4. Solution Procedure

4.1. *Approximation Method*

One of the most applied methods to solve the partial differential governing equations of continuous systems is approximate methods. Rayleigh-Ritz's approach as one of such methods is an extension of Rayleigh's energy method that can be used only for computing the fundamental frequency; however, Rayleigh-Ritz method can be employed to find all the frequencies. According to this method for a conservative system, the maximum potential and kinetic energies are equal which is accompanied by the fact that natural modes execute harmonic motions. Consequently, with defining ω as the frequency of the system, the maximum energy terms are as follows:

$$T_{max} = \frac{1}{2}\omega^2\left(\int_0^L I_{11}W^2\,dx + MW^2(L)\right) \quad (23)$$

$$U_{max} = \frac{1}{2}\int_0^L (S_{11} + S_{22})\,(\frac{d^2W}{dx^2})^2 dx \quad (24)$$

In which, the coefficients are:

$$I_{11} = \int_A \rho(z)dA \quad (25)$$

$$S_{11} = \int_A G(z)\,l^2 dA \quad (26)$$

$$S_{22} = \int_A E(z)z^2 dA \quad (27)$$

By separating lateral displacement ($w(x,t) = W(x)T(t)$), Rayleigh's quotient (square of the frequency) ($R[W(x)]$) easily can be defined as follows: ($W(x)$ is the amplitude).

$$R[W(x)] = {\omega_n}^2 = \frac{\int_0^L (S_{11}+S_{22})(\frac{d^2W}{dx^2})^2 dx}{\int_0^L I_{11}W^2 dx + MW^2(L)} \quad (28)$$

4.2. *Rayleigh-Ritz method*

Rayleigh-Ritz method is applied in order to appraised frequencies of different modes of vibration. In this method, the actual frequency for each mode is smaller than the appraised one. The method consists of selecting a trial family of admissible functions satisfying the homogenous and geometric boundary conditions and constructing a linear combination for mode shape functions as follows:

$$w_n = \sum_{i=1} a_i u_i \quad (29)$$

where the u_i are known functions and a_i are the unknown coefficients to be computed. For each mode, the mode shape function is substituted in Rayleigh's quotient so as to render the quotient stationary, which means that it is required to minimize the estimate. This minimization is done with respect to the unknown coefficients.

$$\frac{\partial R(W_n)}{\partial a_i} = 0 \quad (30)$$

Manifesting some mathematical operations leads to the Galerkin's equations:

$$\sum_{i=1}^{n}\left(K_{ij} - {\omega_n}^2 m_{ij}\right)a_i = 0, \quad r = 1,2,\dots,n \quad (31)$$

where stiffness and mass matrices are defined as follows:

$$K_{ij} = \int_0^L (S_{11} + S_{22}) \frac{d^2u_i}{dx^2} \frac{d^2u_j}{dx^2} dx \quad (32)$$

$$m_{ij} = \int_0^L I_{11}\, u_i u_j\, dx + M\, u_i(L)\, u_j(L) \quad (33)$$

The trial functions satisfying the homogenous boundary conditions are supposed to be polynomial functions.

$$u_i = \left(\frac{x}{L}\right)^{i+1} \quad , i = 1,2, \ldots \quad (34)$$

Exerting the above functions in the quotient and solving the frequency equation calculated from the Galerkin's equations will result in the frequencies of the system.

5. Numerical Results and Discussion

The functionally graded micro-cantilever beam inspected in this paper is a mixture of steel and alumina (aluminium oxide), at which its properties vary through the thickness according to a power-law. The lower surface is pure metal, and the upper surface is pure alumina. The mechanical properties of the two constituents are expressed in Table 1. The beam length is $L =$ 10,000 micrometers and its width is $L =$ 1,000 micrometers.

Applying the following relation $\widehat{\omega} = \omega L^2 \sqrt{\rho_a A / E_a I}$, where $I = bh^3/12$ is the second moment of inertia of the beam, and A is the area of the cross-section; the non-dimensional frequency is obtained. In accordance with experimental tests reported by Lame, the material length scale parameter (l) is taken 15 micrometers. For verification, the results are compared with those of technical references.

In Table 2, by neglecting the material length scale parameter $(l = 0)$, for the modified couple stress theory and assuming the mass ratio and power index, both equal to zero $(R, k = 0)$, comparison with a technical report is done, leading to a good level of accuracy.

Pursuant to Table 2. It can be observed that current results are verified by technical literature. By accounting and neglecting the material length-scale parameter and putting the power index equal to zero, the results are verified. In Tables 3-5 non-dimensional frequency of a micro-cantilever Euler-Bernoulli beam, carrying an attached mass, and using the modified couple stress theory for dissimilar values of power indices are displayed.

The results are reported based on the varying mass ratio of the system (ratio of the mass of the attached mass to the mass of the beam), in which, numerical results for the first mode are portrayed in Table 3, the second mode in Table 4, and the third mode in Table 5. Regularly the change in the values of non-dimensional frequencies is expected by the growth of the power index. Tables 3, 4 and 5 reveal the fact that through increasing the power index, non-dimensional frequency decreases and this is observable for dissimilar values of power index ($K =$ 0.0.,0.1,0.2,0.5,1,2,5,10). The second point that is detectable from Tables 3, 4 and 5 is the influence of mass ratio. As the attached mass is heavier, the non-dimensional frequency decreases and this decrement becomes more intense in higher modes of vibration.

Table 1. Mechanical properties

Property	Steel	Alumina
ρ (Kg/m^3)	7800	3960
E(GPa)	210	390

Table 2. Comparison of the non-dimensional frequencies

R	Rao	MCST $(l = 0)$	MCST $(l \neq 0)$
0.01	3.4299	3.4477	3.6305
0.1	2.9687	2.9678	3.1252
1	1.5575	1.5573	1.6399
10	0.5417	0.5414	0.5701
100	0.1731	0.1730	0.1822

Table 3. Non-dimensional natural frequencies of a micro-cantilever beam. (First Mode)

0	$K = 0.0$	$K = 0.1$	$K = 0.2$	$K = 0.5$	$K = 1$	$K = 2$	$K = 5$	$K = 10$
0	3.7025	3.4546	3.2715	2.9314	2.6628	2.4457	2.2419	2.1285
0.01	3.6305	3.3928	3.2165	2.8880	2.6276	2.4165	2.2174	2.1063
0.1	3.1252	2.9508	2.8187	2.5666	2.3618	2.1924	2.0276	1.9320
1	1.6399	1.5828	1.5379	1.4491	1.3743	1.3107	1.2419	1.1955
3	1.0139	0.9837	0.9599	0.9127	0.8732	0.8397	0.8021	0.7749
5	0.7971	0.7743	0.7563	0.7207	0.6910	0.6660	0.6374	0.6164
7.5	0.6558	0.6374	0.6230	0.5943	0.5705	0.5504	0.5274	0.5103
10	0.5701	0.5543	0.5419	0.5173	0.4968	0.4796	0.4599	0.4451
30	0.3317	0.3227	0.3157	0.3017	0.2901	0.2804	0.2692	0.2607
50	0.2573	0.2504	0.2450	0.2342	0.2253	0.2178	0.2091	0.2025
100	0.1822	0.1773	0.1735	0.1659	0.1596	0.1543	0.1482	0.1435

Table 4. Non-dimensional natural frequencies of a micro-cantilever beam. (Second Mode)

R	$K = 0.0$	$K = 0.1$	$K = 0.2$	$K = 0.5$	$K = 1$	$K = 2$	$K = 5$	$K = 10$
0	23.2030	21.6499	20.5018	18.3709	16.6873	15.3271	14.0494	13.3393
0.01	22.7665	21.2738	20.1670	18.1058	16.4717	15.1478	13.8993	13.2021
0.1	20.3822	19.1507	18.2307	16.5018	15.1178	13.9868	12.9016	12.2811
1	17.1118	16.0291	15.2276	13.7378	12.5600	11.6081	10.7040	10.1897
3	16.5534	15.4703	14.6694	13.1827	12.0087	11.0607	10.1666	9.6647
5	16.4297	15.3455	14.5439	13.0561	11.8810	10.9322	10.0386	9.5389
7.5	16.3662	15.2813	14.4792	12.9905	11.8147	10.8651	9.9716	9.4728
10	16.3341	15.2487	14.4464	12.9571	11.7809	10.8308	9.9372	9.4390
30	16.2689	15.1826	14.3797	12.8892	11.7118	10.7607	9.8669	9.3695
50	16.2557	15.1692	14.3661	12.8754	11.6978	10.7464	9.8525	9.3554
100	16.2458	15.1592	14.3560	12.8651	11.6872	10.7356	9.8417	9.3447

Table 5. Non-dimensional natural frequencies of a micro-cantilever beam. (Third Mode)

R	$K = 0.0$	$K = 0.1$	$K = 0.2$	$K = 0.5$	$K = 1$	$K = 2$	$K = 5$	$K = 10$
0	64.9690	60.6203	57.4058	51.4390	46.7250	42.9163	39.3389	37.3505
0.01	63.7820	59.5952	56.4918	50.7133	46.1332	42.4232	38.9253	36.9724
0.1	58.4624	54.7989	52.0761	46.9892	42.9419	39.6513	36.5167	34.7387
1	53.5948	50.0818	47.4841	42.6610	38.8512	35.7739	32.8721	31.2447
3	52.9576	49.4404	46.8403	42.0139	38.2018	35.1226	32.2264	30.6111
5	52.8224	49.3036	46.7024	41.8741	38.0602	34.9793	32.0831	30.4699
7.5	52.7538	49.2341	46.6323	41.8028	37.9878	34.9059	32.0095	30.3973
10	52.7192	49.1990	46.5969	41.7668	37.9512	34.8687	31.9722	30.3604
30	52.6496	49.1283	46.5255	41.6941	37.8771	34.7934	31.8965	30.2858
50	52.6356	49.1141	46.5111	41.6794	37.8622	34.7782	31.8812	30.2707
100	52.6250	49.1034	46.5003	41.6684	37.8510	34.7668	31.8697	30.2593

In Table 6, numerical results for the non-dimensional frequency of the FG micro-beam with respect to the varying position of the attached mass are depicted. Effect of the relative position of the attached mass and the mass ratio for the first, second and third modes of vibrations are presented. x_{am}/L refers to the position of the attached mass with respect to the beam length. The power index is supposed to be zero ($k = 0$).

Tables 7 and 8 exhibits the same results for $k = 1$ and $k = 10$. pursuant to Tables 6, 7, and 8; regardless of the mass ratio, the frequency decreases as the mass reaches the free end of the beam. Furthermore, increment in mass ratio makes the system to vibrate with less frequency.

Figure 2 persuades the variation of non-dimensional frequencies of the first mode of vibration with respect to different mass ratios, in which three power index values are adopted ($k = 0, 1, 10$). The variations are such that besides the decrement of frequencies with increment in mass ratios, the gradient of the changes is gentle, means that until reaching the ratio $R = 10$, a sharp decrement can be observed, however, for larger ratios, the gradient is not as intense as before. Eventually, for ratios over 50, the decrement and change could be neglected; better means that the dynamical behavior of the system is independent of inertia of the attached mass. In addition, it can be readily observed that for other values of power index, the above inferences are derived.

The variations of non-dimensional frequencies of the first mode of vibration with respect to power index and for six different mass ratios are portrayed in Fig. 3. Based on this figure, increment in power index leads to decrement in the frequencies, when the mass ratio is smaller than 1 ($R < 1$), for the intervals $0 < k < 2$, significant changes take place, while for $k > 2$, the dependency of the frequencies is going to diminish and smooth variations will be experienced. The effects of the mass ratios appear in the way that for ratios larger than one. The variation profile corresponds to a straight line, which means that if a heavy mass in comparison to the beam is attached, the system will vibrate regardless of the magnitude of the power index and the frequencies are such small that it does not matter whether power index is 0.1 or 10. So, the substantial effects of the mass ratios are again observed.

Figure 4 indicates the variations of the non-dimensional frequency with respect to the mass ratio, and assuming $k = 0$, it is accompanied by the consideration of four different positions of the attached mass as well.

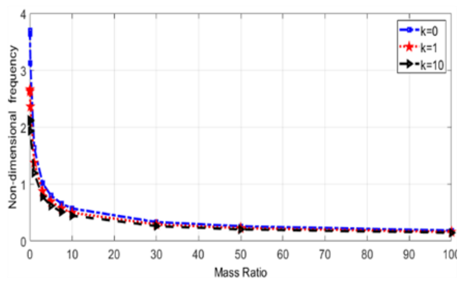

Fig 2. Variation of the frequency with the mass ratio for different power indices

Table 6. Non-dimensional natural frequencies of a micro-cantilever beam with respect to relative attached mass position. (k=0)

R	Mode No.	X_{am}/L=0.25	X_{am}/L=0.5	X_{am}/L=0.75	X_{am}/L=1
0.01	$n=1$	3.7018	3.6940	3.6708	3.6305
	$n=2$	23.1223	22.9711	23.1946	22.7665
	$n=3$	64.2982	64.9686	64.5392	63.7820
0.1	$n=1$	3.6955	3.6195	3.4183	3.1252
	$n=2$	22.4114	21.2194	23.1299	20.3822
	$n=3$	59.2055	64.9649	61.3967	58.4624
1	$n=1$	3.6326	3.0446	2.2386	1.6399
	$n=2$	17.1691	14.9890	22.8754	17.1118
	$n=3$	43.6551	64.9524	52.2481	53.5948
3	$n=1$	3.4949	2.3508	1.4856	1.0139
	$n=2$	12.3594	12.4169	22.7620	16.5534
	$n=3$	39.3497	64.9477	49.4167	52.9576
5	$n=1$	3.3621	1.9793	1.1896	0.7971
	$n=2$	10.3784	11.6906	22.7293	16.4297
	$n=3$	38.3757	64.9464	48.7006	52.8224
7.5	$n=1$	3.2055	1.6936	0.9884	0.6558
	$n=2$	9.0824	11.2899	22.7111	16.3662
	$n=3$	37.8793	64.9457	48.3187	52.7538
10	$n=1$	3.0610	1.5038	0.8636	0.5701
	$n=2$	8.3278	11.0793	22.7015	16.3341
	$n=3$	37.6293	64.9453	48.1212	52.7192
30	$n=1$	2.2835	0.9156	0.5079	0.3317
	$n=2$	6.5903	10.6364	22.6810	16.2689
	$n=3$	37.1270	64.9445	47.7128	52.6496
50	$n=1$	1.8809	0.7172	0.3949	0.2573
	$n=2$	6.2255	10.5442	22.6767	16.2557
	$n=3$	37.0262	64.9444	47.6288	52.6356
100	$n=1$	1.3941	0.5115	0.2800	0.1822
	$n=2$	5.9591	10.4743	22.6734	16.2458
	$n=3$	36.9506	64.9443	47.5654	52.6250

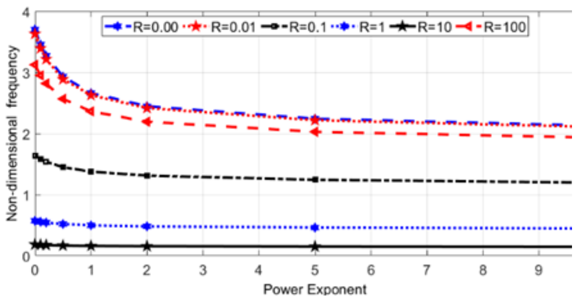

Fig 3. Variation of the frequency with material graduation for different mass ratios

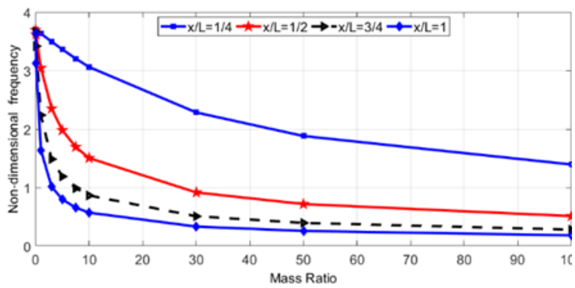

Fig 4. Variation of the frequency with mass ration for different relative positions k = 0

Confirming the results are discussed in Fig. 2, it can be concluded that as the attached mass approaches the free end, the decrements of natural frequencies are sharper and more substantial-frequency drops are seen.

Consequently, it is concluded that the inertia influence of the attached mass for vibration diminishes, as the mass gets closer to the clamped end. This inference can be estimated from Fig. 5, too. This Figure reveals the non-dimensional changes with the location of the attached mass. It is clear that as the attached mass approaches the free end, the system vibrates with smaller frequencies and as the power index is assumed larger number, the effects of the attached mass and its relative position are going to be diminished.

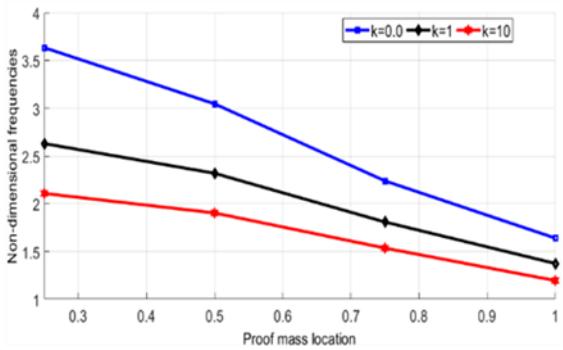

Fig 5. Variation of the frequency with the attached mass location for different power indices

Table 7. Non-dimensional natural frequencies of a micro-cantilever beam with respect to relative attached mass position. (k=1)

R	Mode No.	X_{am}/L=0.25	X_{am}/L=0.5	X_{am}/L=0.75	X_{am}/L=1
0.01	$n=1$	2.6624	2.6586	2.6474	2.6276
	$n=2$	16.6482	16.5743	16.6832	16.4717
	$n=3$	46.3983	46.7247	46.5153	46.1332
0.1	$n=1$	2.6594	2.6222	2.5199	2.3618
	$n=2$	16.3011	15.6735	16.6503	15.1178
	$n=3$	43.7769	46.7228	44.8799	42.9419
1	$n=1$	2.6289	2.3181	1.8083	1.3743
	$n=2$	13.4439	11.6452	38.6579	12.5600
	$n=3$	33.1855	46.7146	16.4889	38.8512
3	$n=1$	2.5616	1.8894	1.2540	0.8732
	$n=2$	10.1257	9.4802	16.3947	12.0087
	$n=3$	29.1175	46.7106	36.1089	38.2018
5	$n=1$	2.4956	1.6305	1.0174	0.6910
	$n=2$	8.5457	8.7943	16.3641	11.8810
	$n=3$	28.1108	46.7094	35.4038	38.0602
7.5	$n=1$	2.4156	1.4182	0.8516	0.5705
	$n=2$	7.4384	8.3993	16.3463	11.8147
	$n=3$	27.5886	46.7087	35.0168	37.9878
10	$n=1$	2.3389	1.2713	0.7471	0.4968
	$n=2$	6.7605	8.1868	16.3366	11.7809
	$n=3$	27.3238	46.7083	34.8137	37.9512
30	$n=1$	1.8650	0.7918	0.4431	0.2901
	$n=2$	5.0582	7.7287	16.3156	11.7118
	$n=3$	26.7890	46.7075	34.3869	37.8771
50	$n=1$	1.5759	0.6235	0.3451	0.2253
	$n=2$	4.6677	7.6316	16.3111	11.6978
	$n=3$	26.6815	46.7073	34.2981	37.8622
100	$n=1$	1.1941	0.4464	0.2451	0.1596
	$n=2$	4.3778	7.5574	16.3076	11.6872
	$n=3$	26.6008	46.7072	34.2306	37.8510

6. Conclusions

In the present study, free lateral vibration analysis of the bio-micro-FG beam that carries a movably attached mass is established. Non-classical constitutive terms are applied in order to strain density function. In the absence of the attached mass; the new model which is based on the modified couple stress theory, predicts the frequencies a bit smaller than the classical theory (for example for a classical model with$R = 0.01$, $\hat{\omega} = 3.4477$, meanwhile applying the non-classical effect frequency is 3.6305); meanwhile, the attached mass remarkably decreases the frequency of the system. In detail, when the attached mass reaches 10 times the mass of the system solely, the frequency decreases close to 80%. Furthermore ,through passing the mentioned Rvalue ($R = 10$), behavior of the entire system is almost independent and vibrations are on the wane regime. Results show that the material length scale parameter, power index and relative position of the attached mass play a major role in the dynamic behavior of FG bio-micro-structures and the presence of an attached mass demonstrates the structural damping effect in the system, exerting direct and explicit influence on vibrational behavior. This effect caused by the attached mass is dependent on the position of the mass along the length of the beam as well. Consequently, it can be realized that a decent and efficient biological laboratory set-up can be devised employed a proper power-law index, and a decent relative position of the attached mass. To put it simple, the material type of bio-sensor and location of the blood/enzyme sample are amongst the crucial factors through the analysis and application of such novel bio-micro-systems. Finally, it is essential to mention that using the proposed model, rapid disease/malfunction detection (diagnosis), is affordable. Addressing key factors of material profile variations and geometrical placement of the sample decent non-classical theorems will lead to eye-catching achievements in clinical diagnostics and biological sciences.

Table 8. Non-dimensional natural frequencies of a micro-cantilever beam with respect to relative attached mass position. (k=10)

R	Mode No.	Xam/L=0.25	Xam/L=0.5	Xam/L=0.75	Xam/L=1
0.01	$n=1$	2.1283	2.1259	2.1188	2.1063
	$n=2$	13.3146	13.2678	13.3367	13.2021
	$n=3$	37.1439	37.3503	37.2178	36.9724
0.1	$n=1$	2.1264	2.1029	2.0369	1.9320
	$n=2$	13.0950	12.6840	13.3155	12.2811
	$n=3$	35.4455	37.3491	36.1524	34.7387
1	$n=1$	2.1071	1.9031	1.5354	1.1955
	$n=2$	11.1985	9.7382	13.1988	10.1897
	$n=3$	27.4987	37.3431	31.4744	31.2447
3	$n=1$	2.0646	1.5985	1.0965	0.7749
	$n=2$	8.7042	7.8932	13.1193	9.6647
	$n=3$	23.7861	37.3396	29.2048	30.6111
5	$n=1$	2.0226	1.4013	0.8982	0.6164
	$n=2$	7.4017	7.2619	13.0913	9.5389
	$n=3$	22.7987	37.3384	28.5349	30.4699
7.5	$n=1$	1.9711	1.2327	0.7561	0.5103
	$n=2$	6.4471	6.8867	13.0745	9.4728
	$n=3$	22.2776	37.3377	28.1591	30.3973
10	$n=1$	1.9211	1.1126	0.6653	0.4451
	$n=2$	5.8446	6.6811	13.0652	9.4390
	$n=3$	22.0115	37.3374	27.9595	30.3604
30	$n=1$	1.5905	0.7049	0.3972	0.2607
	$n=2$	4.2475	6.2291	13.0445	9.3695
	$n=3$	21.4717	37.3366	27.5347	30.2858
50	$n=1$	1.3683	0.5573	0.3099	0.2025
	$n=2$	3.8567	6.1317	13.0400	9.3554
	$n=3$	21.3628	37.3364	27.4454	30.2707
100	$n=1$	1.0546	0.4003	0.2203	0.1435
	$n=2$	3.5606	6.0571	13.0365	9.3447
	$n=3$	21.2811	37.3363	27.3773	30.2593

References

[1] Jha D, Kant T, Singh R. A critical review of recent research on functionally graded plates. *Composite Structures* 2013; 96: 833-49.

[2] Ghanbari A, Babaei A. The new boundary condition effect on the free vibration analysis of micro-beams based on the modified couple stress theory. *International Research Journal of Applied and Basic Sciences* 2015; 9(3): 274-9.

[3] Babaei A, Yang CX. Vibration analysis of rotating rods based on the nonlocal elasticity theory and coupled displacement field. *Microsystem Technologies* 2019; 25(3): 1077-85.

[4] Babaei A, Ahmadi I. Dynamic vibration characteristics of non-homogenous beam-model MEMS. *Journal of Multidisciplinary Engineering Science Technology* 2017; 4(3): 6807-14.

[5] Babaei A, Rahmani A. On dynamic-vibration analysis of temperature-dependent Timoshenko microbeam possessing mutable nonclassical length scale parameter. *Mechanics of Advanced Materials and Structures* 2018: 1-8.

[6] Babaei A, Rahmani A, Ahmadi I. Transverse vibration analysis of nonlocal beams with various slenderness ratios, undergoing thermal stress. *Archive of Mechanical Engineering* 2019.

[7] Babaei A. Longitudinal vibration responses of axially functionally graded optimized MEMS gyroscope using Rayleigh–Ritz method, determination of discernible patterns and chaotic regimes. *SN Applied Sciences* 2019; 1(8): 831.

[8] Chen W, Lv C, Bian Z. Free vibration analysis of generally laminated beams via state-space-based differential quadrature. *Composite Structures* 2004; 63(3): 417-25.

[9] Xiang H, Yang J. Free and forced vibration of a laminated FGM Timoshenko beam of variable thickness under heat conduction. *Composites Part B: Engineering* 2008; 39(2): 292-303.

[10] Lü C, Lim CW, Chen W. Size-dependent elastic behavior of FGM ultra-thin films based on generalized refined theory. *International Journal of Solids and Structures* 2009; 46(5): 1176-85.

[11] Amar LHH, Kaci A, Yeghnem R, Tounsi A. A new four-unknown refined theory based on modified couple stress theory for size-

dependent bending and vibration analysis of functionally graded micro-plate. *Steel and Composite Structures* 2018; 26(1): 89-102.
[12] Pradhan K, Chakraverty S. Free vibration of Euler and Timoshenko functionally graded beams by Rayleigh–Ritz method. *Composites Part B: Engineering* 2013; 51: 175-84.
[13] Aghazadeh R, Cigeroglu E, Dag S. Static and free vibration analyses of small-scale functionally graded beams possessing a variable length scale parameter using different beam theories. *European Journal of Mechanics-A/Solids* 2014; 46: 1-11.
[14] Jafari-Talookolaei R-A, Ebrahimzade N, Rashidi-Juybari S, Teimoori K. Bending and vibration analysis of delaminated Bernoulli–Euler micro-beams using the modified couple stress theory. *Scientia Iranica* 2018; 25(2): 675-88.
[15] Ansari R, Gholami R, Sahmani S. Free vibration analysis of size-dependent functionally graded microbeams based on the strain gradient Timoshenko beam theory. *Composite Structures* 2011; 94(1): 221-8.
[16] Asghari M, Ahmadian M, Kahrobaiyan M, Rahaeifard M. On the size-dependent behavior of functionally graded micro-beams. *Materials & Design (1980-2015)* 2010; 31(5): 2324-9.
[17] Ansari R, Gholami R, Shojaei MF, Mohammadi V, Sahmani S. Bending, buckling and free vibration analysis of size-dependent functionally graded circular/annular microplates based on the modified strain gradient elasticity theory. *European Journal of Mechanics-A/Solids* 2015; 49: 251-67.
[18] Babaei A, Noorani M-RS, Ghanbari A. Temperature-dependent free vibration analysis of functionally graded micro-beams based on the modified couple stress theory. *Microsystem Technologies* 2017: 1-12.
[19] Shafiei N, Mousavi A, Ghadiri M. Vibration behavior of a rotating non-uniform FG microbeam based on the modified couple stress theory and GDQEM. *Composite Structures* 2016; 149: 157-69.
[20] Ansari R, Oskouie MF, Gholami R, Sadeghi F. Thermo-electro-mechanical vibration of postbuckled piezoelectric Timoshenko nanobeams based on the nonlocal elasticity theory. *Composites Part B: Engineering* 2016; 89: 316-27.
[21] Farajpour A, Ghayesh MH, Farokhi H. Super and subcritical nonlinear nonlocal analysis of NSGT nanotubes conveying nanofluid. *Microsystem Technologies* 2019: 1-15.
[22] Mohammadimehr M, Mohammadi Hooyeh H, Afshari H, Salarkia M. Size-dependent Effects on the Vibration Behavior of a Timoshenko Microbeam subjected to Pre-stress Loading based on DQM. *Mechanics of Advanced Composite Structures* 2016; 3(2): 99-112.
[23] Arabghahestani M, Karimian S. Molecular dynamics simulation of rotating carbon nanotube in uniform liquid argon flow. *Journal of Molecular Liquids* 2017; 225: 357-64.
[24] Fang J, Gu J, Wang H. Size-dependent three-dimensional free vibration of rotating functionally graded microbeams based on a modified couple stress theory. *International Journal of Mechanical Sciences* 2018; 136: 188-99.
[25] Khaniki HB, Rajasekaran S. Mechanical analysis of non-uniform bi-directional functionally graded intelligent micro-beams using modified couple stress theory. *Materials Research Express* 2018; 5(5): 055703.
[26] Jia X, Ke L, Zhong X, Sun Y, Yang J, Kitipornchai S. Thermal-mechanical-electrical buckling behavior of functionally graded micro-beams based on modified couple stress theory. *Composite Structures* 2018; 202: 625-34.